Clays and Clay Minerals, Vol. 53, No. 5, 423–439, 2005.

ILLITE-SMECTITE MIXED-LAYER MINERALS IN THE HYDROTHERMAL ALTERATION OF VOLCANIC ROCKS: I. ONE-DIMENSIONAL XRD STRUCTURE ANALYSIS AND CHARACTERIZATION OF COMPONENT LAYERS

ATSUYUKI INOUE[1,*], BRUNO LANSON[2], MARIA MARQUES-FERNANDES[2], BORIS A. SAKHAROV[2,3], TAKASHI MURAKAMI[4], ALAIN MEUNIER[5] AND DANIEL BEAUFORT[5]

[1] Department of Earth Sciences, Chiba University, Chiba 263-8522, Japan
[2] LGIT-Maison des GéoScience, BP53, Université de J. Fourier, 38041 Grenoble Cedex 9, France
[3] Geological Institute, Russian Academy of Sciences, Pyzhevsky per. 7, 119017 Moscow, Russia
[4] Department of Earth and Planetary Science, The University of Tokyo, Tokyo 113-0033, Japan
[5] HydrASA-UMR 6532 CNRS, Université de Poitiers, 40 av. Recteur Pineau, 86022 Poitiers Cedex, France

Abstract—For a series of mixed-layer illite-smectite (I-S) minerals from a drillhole near the Kakkonda geothermal field, one-dimensional structure analysis by X-ray diffraction (XRD) was performed using Ca-saturated specimens in both air-dried and ethylene glycol-solvated states. The expandability characteristics of component layers were also examined by means of alkylammonium exchange and Li saturation. The K content in the illite layers was $1.5-1.7/O_{20}(OH)_4$ in the I-S series from 3 to 85% of I-layer content (% I). The layer charge of the smectite layer varied slightly within the range of $0.3-0.5/O_{10}(OH)_2$ by alkylammonium exchange experiments and the expandability was independent of the beidellite content within a range of 0–0.5 by the Li-saturation test. The degree of long-range ordering represented by Reichweite (R) parameters varied from R0 to R3 *via* R1 and R2 with increase in % I. The I-S samples contained <10% vermiculite as the third component and the vermiculite content tended to decrease with progressive illitization.

In contrast to the smectitic R0 samples (<10% I), more illitic R0 (*e.g.* 35% I) and >R1 I-S samples showed complicated expandability with alkylammonium exchange. The XRD patterns of dodecylammonium-exchanged I-S samples can be interpreted by random interstratification of several types of sub-units such as layer-doublets, layer-triplets and layer-quartets present in the crystallites. This interpretation is consistent with the variation in the occurrence probabilities of layer-multiplets calculated from the junction probabilities and the proportions of layers. Because the interpretation indicates that I-S is a stack of various types of the sub-units, the smectite illitization can be described by a systematic change in the type and proportion of the sub-units constituting crystallites.

Key Words—Alkylammonium Exchange, Expandability, Hydrothermal System, Illite-smectite Mixed-layer Minerals, One-dimensional XRD Structure Analysis.

INTRODUCTION

Sequential smectite-to-illite reaction *via* mixed-layer minerals (referred to hereafter as 'smectite illitization') has been documented in low-temperature crustal environments and is commonly associated with burial diagenesis, low-grade metamorphism, contact metamorphism and hydrothermal alteration. Despite extensive investigation over the last several decades (see the review by Meunier and Velde, 2004), many unresolved points remain, including the crystal chemical models of illite-smectite (I-S) mixed-layered structures and the illitization mechanism. Previous XRD studies of I-S minerals suggested that smectite illitization occurs with a continuous variation in the proportions of smectite (S) and illite (I) layers regardless of geological environment (*e.g.* Hower *et al.*, 1976 for diagenesis; Inoue *et al.*, 1978 for hydrothermal alteration). The sequence of interstratified I-S minerals with different I/S ratios also includes a continuous change in the ordering of layer stacking from smectite-rich R0 I-S to illite-rich R3 I-S, where R is the Reichweite parameter (Jagodzinski, 1949). However, recent transmission electron microscopy (TEM) studies have indicated that smectite, R1 and illite layers are abundant, whereas I-S with other types of orderings (*i.e.* R>1) are rare (Dong *et al.*, 1997; Bauluz *et al.*, 2000 and references therein). Thus the continuous change in proportion of S and I layers and the orderings indicated by XRD investigations contradicted the discontinuous change revealed by TEM observations.

Altaner and Ylagan (1997) and Plançon (2004) argued that there are two ways to describe the layer-stacking sequence of I-S interstratification from a crystallochemical points of view. One is the interstratification of two individual 2:1 layers with homogeneous smectite and illite compositions, respectively. This type of stacking model is called a non-polar 2:1 layer model (Altaner and Ylagan, 1997). The other is to describe it on the basis of stacking of two interlayer-centered

* E-mail address of corresponding author:
atinoue@earth.s.chiba-u.ac.jp
DOI: 10.1346/CCMN.2005.0530501

smectite and illite in which each 2:1 layer has heterogeneous composition, and this is called a polar 2:1 layer model (Altaner and Ylagan, 1997). It is still disputed as to which is the better way to describe the layer-stacking sequence of I and S layers within a crystallite which acts as a coherent unit able to scatter X-rays. Furthermore, the questions of whether or not the third component layer, which is often called a vermiculite or 'high-charged smectite' layer, exists in I-S stacks and whether or not the formation acts as an essential step during smectite illitization are unanswered (*e.g.* Drits *et al*., 1997a; Meunier *et al*., 2000). Finally, since the illitization mechanism is deduced from these basic XRD and TEM data, the mechanistic relations between layer-by-layer, solid-state transformation (SST) and dissolution-crystallization (DC) models are major points of contention (Altaner and Ylagan, 1997).

Both the illitization process and the crystal chemistry of I-S depend on variables in different systems, which include temperature, compositions of fluid and rock and water/rock ratio, in addition to geological time. Among many geological environments mentioned above, hydrothermal alteration is the most appropriate to investigate illitization because we can minimize the effects of precursor materials on illitization in hydrothermally altered volcanic rocks. Although illitization in diagenesis of pelitic rocks is most common, the rocks contain precursor smectite, detrital illite and other phyllosilicates. Variability in the inherited characteristics of smectite formed during earlier periods of weathering may influence later illitization during burial diagenesis. The time factor may be ignored in the case of I-S formation in hydrothermal alteration because the formation generally takes place over a geologically short period of time in contrast to burial diagenesis.

This study investigates an I-S series which has its origin in hydrothermal alteration, *i.e*. I-S minerals from a drillhole (IT-2) near the Kakkonda active geothermal system, Japan. This field is characterized by constant, high geothermal gradients (~15−20ºC/100 m) up to at least 1700 m, with neither boiling nor circulation of fluids, and no alteration overprint (Inoue *et al*., 2001). The I-S minerals are formed from Miocene to Pleistocene felsic volcaniclastic rocks with a limited range of composition under temperatures similar to the present temperature and nearly constant water/rock ratio (Inoue *et al*., 2001; Inoue *et al*., 2004). The occurrence, bulk mineralogy, fluid geochemistry and isotope characteristics were described in detail in these previous works. More detailed XRD and high-resolution TEM (HRTEM) characterization of selected I-S minerals has been undertaken to elucidate the unresolved points mentioned above and to understand better the mechanism of I-S formation. This work consists of two parts; special attention in the first part is paid to characterizing the expandability behavior of component layers in the Kakkonda I-S series based on one-dimensional XRD structure analysis and supplementary examinations by alkylammonium ion exchange and Li ion-saturation techniques. The results of a HRTEM study are described in part II of this work (Murakami *et al*., 2005).

SAMPLES AND EXPERIMENTAL METHODS

Samples

Eleven samples were selected from an I-S series in felsic volcaniclastic rocks from a drill-core (Hole IT-2) near the Kakkonda active geothermal system, Japan. A summary of sample characteristics is provided in Table 1.

Table 1. Chemical composition, % I and formation temperature of the Kakkonda I-S samples studied (after Inoue *et al*., 2004).

Samples	IT2-214	IT2-320	IT2-435	IT2-580	IT2-635	IT2-645	IT2-656	IT2-690	IT2-700	IT2-756	IT2-919
Tetrahedral Si	3.93	4.00	3.90	3.75	3.71	3.48	3.47	3.37	3.44	3.43	3.36
Al	0.07	0.00	0.10	0.25	0.29	0.52	0.53	0.63	0.56	0.57	0.64
Octahedral Al	1.37	1.33	1.32	1.62	1.66	1.83	1.77	1.84	1.84	1.79	1.70
Fe^{3+}	0.32	0.26	0.35	0.19	0.13	0.08	0.10	0.08	0.06	0.01	0.10
Mg	0.23	0.32	0.28	0.19	0.19	0.09	0.10	0.07	0.09	0.22	0.25
Interlayer Ca	0.05	0.02	0.04	0.01	0.06	0.02	0.01	0.01	0.01	0.01	0.00
Na	0.26	0.34	0.34	0.42	0.37	0.30	0.23	0.22	0.22	0.14	0.08
K	0.04	0.08	0.05	0.03	0.17	0.26	0.44	0.44	0.46	0.59	0.68
Layer charge [$/O_{10}(OH)_2$]	0.46	0.51	0.45	0.40	0.42	0.57	0.64	0.69	0.64	0.73	0.74
% I	5	13	2	4	45	45+60*	62	57	62	75	>95
Formation temp. (ºC)**	68	89	111	143	154	156	158	164	166	175	205
Impurities***	pl	opal, cpt	opal, qz, sid	qz	pl, qz	qz	qz	qz	qz		qz, pl, cor

* A mixture of two phases
** The temperatures are those observed at present
*** pl: plagioclase, opal: opal-CT, cpt: clinoptilolite, qz: quartz, sid: siderite, ill: illite, ab: albite, cor: corrensite

XRD diffraction structure analysis

Structure analysis of seven samples (435 m, 580 m, 635 m, 645 m, 690 m, 700 m and 756 m) was carried out using Ca-saturated specimens to minimize the hydration heterogeneity of expandable interlayers. Separated clay fractions (<2 μm) were first saturated with Ca ions and then the homoionic exchanged specimens were X-rayed in two states, air-dried (at controlled relative humidity of 40%) and ethylene glycolated (saturated with ethylene glycol (EG) atmosphere at 70ºC overnight). The XRD patterns were recorded using a Bruker D5000 diffractometer equipped with a Kevex Si (Li) solid-state detector and CuKα radiation. Intensities were recorded at 0.04º2θ steps, from 2−50º2θ, using a counting time of 6 s per step.

A program developed by Drits *et al*. (1997a) and Sakharov *et al*. (1999) was used to fit experimental XRD profiles. Many parameters necessary for simulating XRD profiles were set as by Claret *et al*. (2004). We assumed the existence of three component layers, illite (I), smectite (S) and vermiculite (V) each composed of non-polar 2:1 layers in the simulations. The S layer is defined as a fully expandable interlayer with 2 H_2O molecules at 40% relative humidity or 2 EG molecules when the interlayer site is occupied by homoionic Ca ions. The V layer is defined as a partly expandable interlayer with 1 H_2O or 1 EG molecule and the I layer as a non-expandable interlayer without H_2O or EG molecules (Drits *et al*., 1997a; Meunier *et al*., 2000). The amount and position of interlayer species such as H_2O and EG molecules in addition to fixed K ions were considered as variable parameters during the fitting process. The Fe contents of octahedral sheets were also optimized during fitting. The accuracy of profile fitting was assessed by means of the residual factor (*RWP*) between experimental and simulated intensities at 2−50º2θ (Howard and Preston, 1989).

Alkylammonium exchange

Expandability (or layer charge) characteristics of component layers in I-S were also examined using two, C_{12}-alkylammonium (dodecylammonium)- and C_{18}-alkylammonium (octadecylammonium)-exchanged, specimens. Following the protocol described by Wilson (1987), ~15 mL of pH-adjusted alkylammonium chloride solution (0.1 M for C_{12}-alkylammonium and 0.05 M for C_{18}-alkylammonium) were added to ~20 mg of Na-saturated, freeze-dried powder specimens and heated in an oil bath at 65ºC for 3 days. Excess alkylammonium chloride was removed by repeated washing with 1:1 ethanol/water and pure ethanol followed by centrifugation; the paste was spread over a glass slide and kept in a vacuum desiccator. The reproducibility was checked by two mutually independent experiments.

The XRD patterns of alkylammonium (AL)-exchanged specimens were recorded using a Rigaku RAD-IB diffractometer with monochromatized CuKα radiation. Intensities were recorded at steps of 0.01º2θ, from 2 to 33º2θ, using a counting time of 4 s per step. Peak decomposition was performed on experimental XRD profiles of C_{12}-AL-exchanged specimens over 2−12º2θ using a DECOMPXR program developed by Lanson (1997).

For comparison, vermiculite (Palabora, South Africa), two rectorite samples (Goto and Ohara, Japan) and another I-S series (Shinzan, Japan) were examined. The average layer charge of the Palabora vermiculite is $0.83/O_{10}(OH)_2$ based on data of Inoue (1984). The Goto rectorite is the same material as that studied by Lagaly (1979), though our sample contains illite and pyrophyllite as impurities. The formula of Ohara rectorite is $(K_{0.92}Na_{0.10}Ca_{0.23})(Al_{3.86}Fe^{3+}_{0.07}Mg_{0.09}Ti_{0.01})(Si_{6.52}Al_{1.48})O_{20}(OH)_4$ (Y. Shinohara, unpublished data). The Shinzan I-S minerals are hydrothermal alteration products of Miocene volcaniclastic rocks, and they have a composition which is similar to those of Kakkonda. The mineralogy of the Shinzan I-S series has been described by Inoue *et al*. (1978), Inoue and Utada (1983) and Inoue *et al*. (1987). The XRD and TEM characteristics have also been reported in many studies (*e.g*. Keller *et al*., 1986; Inoue *et al*., 1990 for XRD; Veblen *et al*., 1990; Amouric and Olives, 1991; Olives *et al*., 2000 for TEM). Thus the Shinzan I-S samples may be regarded as 'reference' hydrothermal I-S minerals.

Li saturation

Distinction between montmorillonitic and beidellitic components in smectite layers was made by Li saturation (Hofmann and Klemen, 1950). A Li-saturated specimen, using a normal LiCl solution, was heated at 300ºC overnight in a ceramic crucible to avoid alkali contamination from glass, then dispersed on a glass slide with water and glycerol saturated after air drying. The proportion of beidellitic component was estimated from comparison of experimental intensity ratios of 1.8 nm and 0.96 nm peaks with those of simulated XRD patterns assuming a segregation structure of beidellite and montmorillonite layers.

RESULTS

Interstratified structure analysis

Comparison of experimental and calculated XRD profiles at air-dried and EG-saturated states is illustrated in Figures 1−6, excluding the 580 m sample. The major structure parameters optimized by fitting are summarized in Table 2. For instance, in the 3-component layers system, the interstratified structure with R = 1 can be described by nine junction probability parameters (*e.g*. P_{SS}, P_{SV}, P_{VS}, P_{VV}, *etc*., where P_{SS} denotes a junction probability of an S layer following an S layer) in addition to three parameters (W_I, W_S and W_V) of the proportion (or occurrence probability) of each component. Only essential parameters are listed in Table 2, and

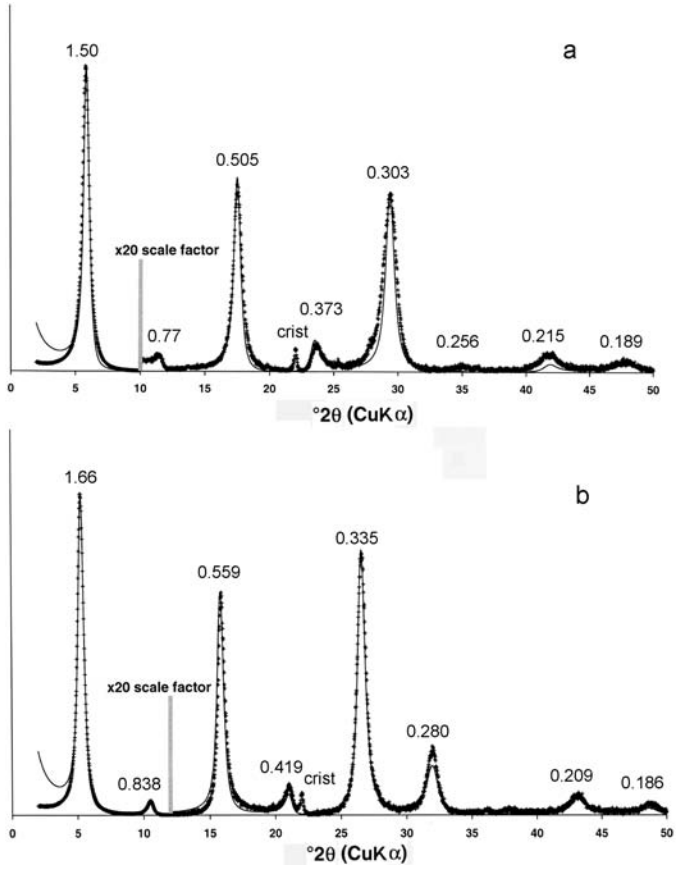

Figure 1. Comparison of experimental (+) and calculated (—) XRD patterns of sample 435 m under Ca-saturated, air-dried (a) and Ca-saturated, EG-saturated (b) conditions. crist: cristobalite. The vertical scale at 2−12°2θ is different from that at 12−50°2θ. The numerical values are the *d* values (nm) of the experimental patterns.

all the other parameters can be easily calculated from those given in the table (Watanabe, 1988; Drits and Tchoubar, 1990). The optimized d_{001} value of the I layer was 0.998 nm for all the samples, those of the S layer were 1.52 nm in the air-dried state and 1.68 nm in the EG-saturated state, and those of the V layer varied from 1.23 to 1.25 nm in the air-dried state and from 1.29 to 1.40 nm in the EG-saturated state (Table 2). The K content of the illite was $1.5-1.7/O_{20}(OH)_4$ in all samples. The optimized Fe contents are consistent with the electron microprobe analyses (Table 1), except for the 435 m sample. The samples studied contain small amounts of impurities as given in Table 1. We did not subtract the contribution of impurities from original the XRD profiles, and thereby the resultant *RWP* values became apparently large from 8.9% to 28.2%. Nevertheless, taking into account agreement in terms of the peak positions and intensities of I-S minerals between the experimental and calculated XRD profiles in both the air-dried and EG-saturated samples, the goodness of fit is satisfactory, as seen in Figures 1−6.

Two samples, 435 m and 580 m are smectite, containing ~10% in total of I and V layers (Figure 1, Table 2). Assuming 1.40 nm for the d_{001} value of the vermiculite layer gave a better fit for the EG-saturated 580 m sample, though the value was greater than the other assumed value of 1.29 nm (Table 2). The reason for the difference in the *d* value is unknown. The optimized Fe content in the octahedral sheets in sample 435 m is noticeably greater than that of the previous chemical analysis (Table 1). Inoue *et al*. (2004) reported that the I-S mineral coexists with siderite at 435 m. The difference in Fe content may be due to the contamination by siderite in the microprobe-analyzed sample, whereas the major impurities of the sample used in the present XRD study are cristobalite and quartz. Calculating the occurrence probabilities of layer doublets, triplets and quartets from the junction probabilities and the proportions of component layers indicates that the SS doublet is mostly dominant within crystallites of samples 435 m and 580 m (Table 3). The occurrence probabilities of SIS and VIV triplets range around 0.02−0.04 in sample 435 m and 0−0.02 in sample 580 m. The mean number of layers (*N*) consisting of X-ray coherent domains is 10 for 435 m and seven for 580 m.

Sample 635 m (Figure 2) is an I-S mixed-layer mineral with R = 0, W_I = 0.35, W_S = 0.65 in the EG-saturated state. The proportion of V layer (W_V) was

Table 2. Optimized structural parameters of Kakkonda I-S mixed-layer minerals

Sample	Measurement conditions		Proportions of *i* layers	d_{001} (nm) — Junction probability —			N	K	Fe	*RWP* (%)
435 m	Ca-AD		R = 0	0.998	1.515	1.25	10	1.5	0.5	22.87
			W_I 0.05							
			W_S 0.9		0.9	0.05				
			W_V 0.05		0.9	0.05				
	Ca-EG		R = 0	0.998	1.68	1.29	10	1.5	0.5	17.11
			W_I 0.05							
			W_S 0.9		0.9	0.05				
			W_V 0.05		0.9	0.05				
580 m	Ca-AD		R = 0	0.998	1.52	1.23	6.5	1.5	0.4	18.91
			W_I 0.03							
			W_S 0.88		0.9	0.05				
			W_V 0.09		0.9	0.05				
	Ca-EG		R = 0	0.998	1.68	1.4	7	1.5	0.4	19.13
			W_I 0.03							
			W_S 0.92		0.92	0.05				
			W_V 0.05		0.92	0.05				
635 m	Ca-AD		R= 0	0.998	1.515	1.25	15	1.5	0.25	19.65
			W_I 0.35							
			W_S 0.55		0.55	0.1				
			W_V 0.1		0.55	0.1				
	Ca-EG		R = 0	0.998	1.675		10	1.5	0.25	13.35
			W_I 0.35							
			W_S 0.65		0.65	0				
			W_V 0		0.65	0				
645 m	Ca-AD	Phase A 83%	R = 0	0.998	1.515	1.25	25	1.5	0.15	16.37
			W_I 0.35							
			W_S 0.55		0.55	0.1				
			W_V 0.1		0.55	0.1				
	Ca-AD	Phase B 17%	R = 1	0.998	1.515	1.25	8	1.5	0.15	
			W_I 0.5							
			W_S 0.4		0.12	0.03				
			W_V 0.1		0.12	0.03				
	Ca-EG	Phase A 80%	R = 0	0.998	1.675		12	1.5	0.15	8.89
			W_I 0.35							
			W_S 0.65		0.65	0				
			W_V 0		0	0				
	Ca-EG	Phase B 20%	R = 1	0.998	1.675		7	1.5	0.15	
			W_I 0.5							
			W_S 0.5		0.15	0				
			W_V 0		0	0				
690 m	Ca-AD		R = 1	0.998	1.515	1.25	15	1.7	0.15	24.44
			W_I 0.55							
			W_S 0.4		0.15	0.05				
			W_V 0.05		0.4	0.05				
	Ca-EG		R = 1	0.998	1.68		15	1.7	0.15	16.13
			W_I 0.55							
			W_S 0.4		0.15	0.05				
			W_V 0.05		0.4	0.05				
700 m	Ca-AD		R1 MPDO R = 2	0.998	1.515	1.25	10	1.7	0	28.22
			W_I 0.6	0.55(SIS), 0.075(SIV), 0.55(VIS), 0.075(VIV) all other probabilities are 0						
			W_S 0.35							
			W_V 0.05							
	Ca-EG		R1 MPDO R = 2	0.998	1.68		10	1.7	0	17.52
			W_I 0.6	0.75(IIS) all other probabilities are 0						
			W_S 0.4							
			W_V 0							
756 m	Ca-AD		R1 MPDO, R2 MPDO R = 3	0.998	1.515	1.25	19	1.5	0	18.23
			W_I 0.85	0.084(SIIS) all other probabilities are 0						
			W_S 0.125							
			W_V 0.025							
	Ca-EG		R1 MPDO, R2 MPDO R = 3	0.998	1.68	1.29	20	1.5	0	24.58
			W_I 0.85	0.084(SIIS) all other probabilities are 0						
			W_S 0.125							
			W_V 0.025							

d_{001}: basal spacing of a given layer; *N*: mean number of layers; W_i: proportion of i layer; K: fixed K ions ($/O_{20}(OH)_4$) in illite interlayer; Ca-AD: Ca-saturated, air-dried; Fe: Fe content ($/O_{20}(OH)_4$) in octahedral sheet; Ca-EG: Ca-saturated, EG-solvated; *RWP*: residual factor; shaded area: junction probabilities; MPDO: maximum possible degree of order

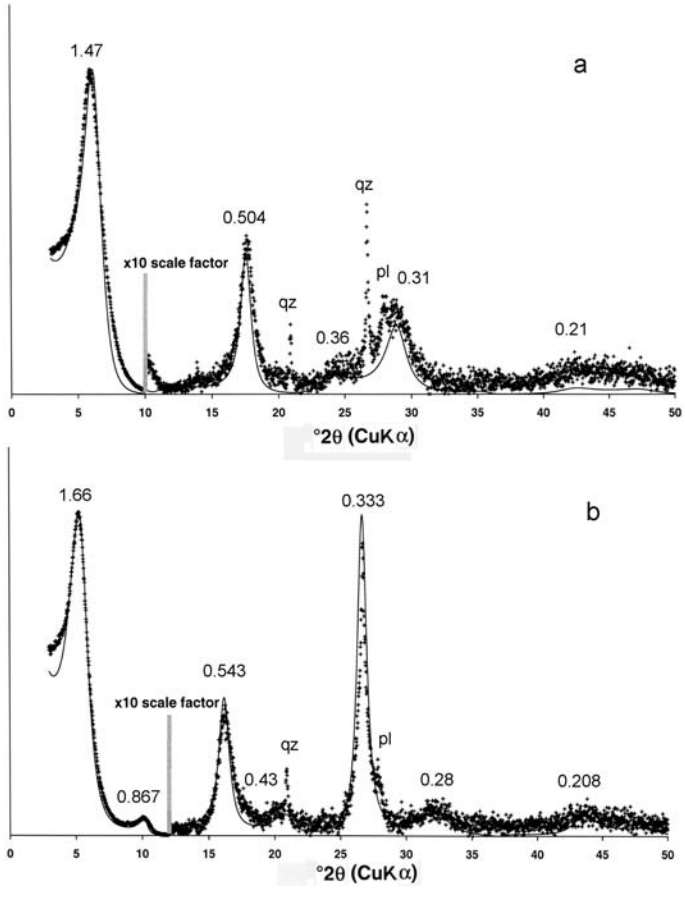

Figure 2. Comparison of experimental (+) and calculated (—) XRD patterns of sample 635 m under Ca-saturated, air-dried (a) and Ca-saturated, EG-saturated (b) conditions. qz: quartz, pl: plagioclase. The numerical values are the *d* values (nm) of the experimental patterns.

estimated to be 0.1 in the air-dried state but was negligible when EG-saturated. In general, the W_V value tended to be equal at EG-solvated and air-dried states in most samples studied. In some samples, the W_V value for the EG-solvated state was smaller than that for the air-dried state (Table 2). The reason was not specified in the present study. In the 635 m sample, the I-layer percentage (% I) or W_I value determined by the present XRD analysis was underestimated in the order of ~10% compared to that determined previously by a convenient saddle/peak ratio technique of Inoue *et al.* (1989) as shown in Table 1. The occurrence probability of an IS doublet (W_{IS}) and SIS triplet (W_{SIS}) increases to 0.23 ($=W_I \cdot W_S$) and 0.15 ($=W_S \cdot W_I \cdot W_S$), respectively, whereas that of an SS doublet decreases to 0.42 (Table 3) compared to those of the 435 m and 580 m samples. The mean number of layers is 15 in the air-dried and 10 in the EG-saturated states.

Sample 645 m (Figure 3) is a mixture of R0 and R1 ordered structures, of which the proportions are 80% and 20%, respectively (Table 2). The W_V value in the R0 phase was estimated to be 0.1, but that in the R1 phase was negligible when EG saturated. For the R0 phase, it is noted that the occurrence probability of an II doublet increases and that of an SS doublet decreases, compared to those of the 635 m sample. For the R1 phase, the occurrence probabilities of II and SS doublets decrease, while those of IS doublets and SIS triplets increase remarkably (Table 3). The estimated mean number of layers is smaller in the R1 phase than in the R0 phase (Table 2). This relationship is distinct in the air-dried state, but becomes ambiguous in the EG-saturated state, as the mean number of layers is eight for the R0 phase and seven for the R1 phase.

Sample 690 m (Figure 4) is an R1 ordered structure with $W_I = 0.55$, $W_S = 0.4$, $W_V = 0.05$ when EG saturated. The occurrence probabilities of W_{IS} ($=W_I \cdot P_{IS}$), W_{IV} ($=W_I \cdot P_{IV}$) and W_{II} ($=W_I \cdot P_{II}$) were calculated to be 0.32, 0.03 and 0.20, respectively (Table 3). Compared to the R1 phase in the 645 m sample, the occurrence probabilities of the IS doublet and SIS triplet decrease and those of the II doublet, IIS triplet and IIIS quartet increase. The mean number of layers is 15 in the air-dried and EG-saturated states.

Structures of samples 700 m and 756 m (Figures 5 and 6) were determined to be R2 and R3 ordered

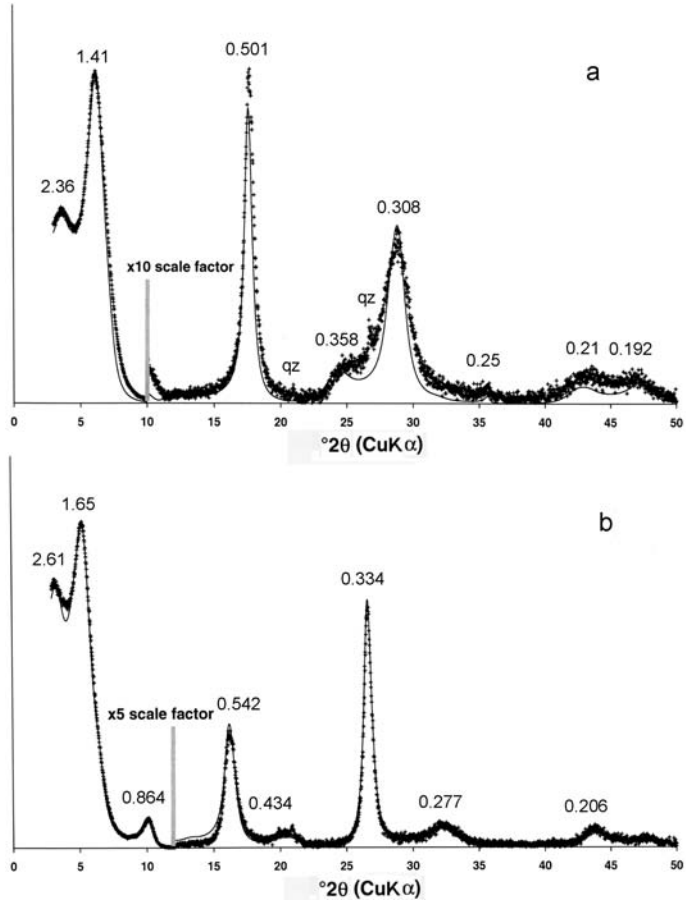

Figure 3. Comparison of experimental (+) and calculated (—) XRD patterns of sample 645 m under Ca-saturated, air-dried (a) and Ca-saturated, EG-saturated (b) conditions. qz: quartz. The numerical values are the *d* values (nm) of the experimental patterns.

structures, respectively, assuming the arrangements of layers with maximum possible degree of ordering (MPDO) (Drits and Tchoubar, 1990). The proportion of V layer is negligible in the two samples. In sample 700 m, the conditions of R2 ordering with R1 MPDO, $W_I = 0.6$, $W_S = 0.4$ when EG saturated lead to $P_{SS} = 0$ and result in W_{IS} (=$W_I \cdot P_{IS}$) = 0.40, W_{II} (=$W_I \cdot P_{II}$) = 0.20 and W_{SIS} (=$W_S \cdot P_{SI} \cdot P_{SIS}$) = 0.10. The occurrence prob-

Table 3. Occurrence probabilities of layers, layer doublets, triplets and quartets in I-S crystallites calculated from junction probabilities for EG-saturated samples.

Layer sequence	435 m R0	580 m R0	635 m R0	645 m R0	645 m R1	690 m R1	700 m R2	756 m R3
I	0.050	0.030	0.350	0.500	0.500	0.550	0.600	0.850
S	0.900	0.880	0.650	0.400	0.500	0.400	0.400	0.125
V	0.050	0.090	0.000	0.100	0.000	0.050	0.000	0.025
II	0.003	0.001	0.123	0.250	0.075	0.203	0.200	0.700
IS	0.045	0.026	0.228	0.200	0.425	0.320	0.400	0.125
IV	0.003	0.003	0.000	0.050	0.000	0.028	0.000	0.026
SS	0.810	0.774	0.423	0.160	0.075	0.060	0.000	0.000
III	0.001	0.000	0.043	0.125	0.011	0.075	0.050	0.576
IIS	0.002	0.001	0.080	0.100	0.064	0.118	0.150	0.103
SIS	0.041	0.023	0.148	0.080	0.361	0.186	0.100	0.018
VIV	0.041	0.000	0.000	0.005	0.000	0.001	0.000	0.000
IIII	0.000	0.000	0.015	0.063	0.002	0.027	0.012	0.466
IIIS	0.000	0.000	0.028	0.050	0.010	0.043	0.037	0.110
SIIS	0.002	0.001	0.052	0.040	0.065	0.069	0.113	0.010
VIIV	0.000	0.000	0.000	0.003	0.000	0.001	0.000	0.000

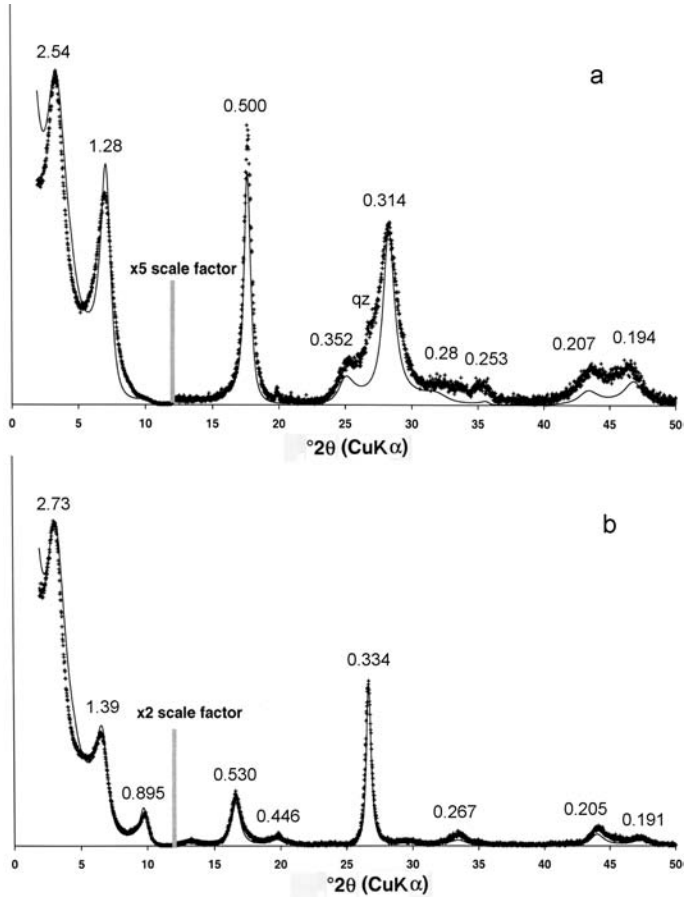

Figure 4. Comparison of experimental (+) and calculated (—) XRD patterns of sample 690 m under Ca-saturated, air-dried (a) and Ca-saturated, EG-saturated (b) conditions. qz: quartz. The numerical values are the *d* values (nm) of the experimental patterns.

ability of an SIIS quartet ($=W_S \cdot P_{SI} \cdot P_{SII} \cdot P_{IIS}$) is 0.11 in the 700 m sample (Table 3). The % I of the 756 m sample was underestimated in the order of 10% compared to the previous estimate (Table 1), probably due to different types of interlayer cations in the specimens used in the two XRD measurements. In the 756 m sample, W_{IS} = 0.13, W_{II} = 0.70 and W_{IV} = 0.03. The occurrence probabilities of an III triplet and an IIII quartet are extremely large compared to the other samples. The mean number of layers is 10 for the 700 m sample and 20 for the 756 m sample.

Alkylammonium exchange

The XRD profiles of the Kakkonda I-S series treated with C_{12}- and C_{18}-AL are illustrated in Figure 7. For comparison, XRD profiles of vermiculite and rectorite are given in Figure 8. The basal spacing of smectite increased from 1.38 nm for sample 214 m to 1.72 nm for sample 580 m for C_{12}-AL-exchanged samples and from 1.77 nm for sample 214 m to 1.9 nm for sample 580 m for C_{18}-AL-exchanged samples. The XRD peaks of AL-exchanged smectite appear to be single and symmetric, suggesting a relatively homogeneous charge distribution. The change in basal spacing corresponds to the monolayer or bilayer arrangement of alkylammonium molecules due to increasing the mean layer charge (Lagaly, 1994). Extremely small d_{001} values (1.38 nm by C_{12}-AL exchange and 1.77 nm by C_{18}-AL exchange) of sample 214 m are caused by the low-charged interlayer (Inoue *et al.*, 2004). Excluding the 214 m sample, the mean values of layer charge tend to increase with increasing depth or the formation temperature, but the extent of the increase is extremely small. The mean layer charge of expandable interlayer in Kakkonda smectite ranges between 0.3 and $0.4/O_{10}(OH)_2$, when the values were evaluated using the calibration curves of Olis *et al.* (1990). The Palabora vermiculite exhibited symmetric, rational series reflections of 2.3 nm by C_{12}-AL exchange and of 3.1 nm by C_{18}-AL exchange (Figure 8). The basal spacing of the Palabora vermiculite is brought about by a paraffin type of arrangement of alkylammonium ions (see the definition of Lagaly, 1994) in high-charge interlayer with $>0.75/O_{10}(OH)_2$ according to Olis *et al.* (1990). Although the XRD structure analysis recognized a maximum V layer of 9% in the air-dried state in the 435 m and 580 m samples (Table 2), a discrete vermiculite phase was not detected by the AL treatments.

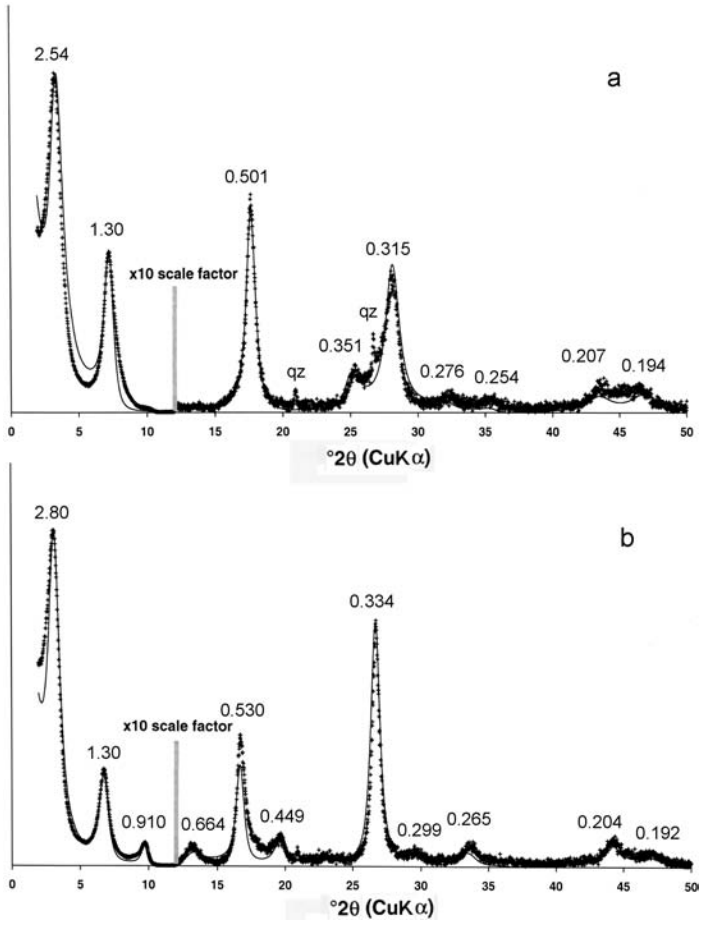

Figure 5. Comparison of experimental (+) and calculated (—) XRD patterns of sample 700 m under Ca-saturated, air-dried (a) and Ca-saturated, EG-saturated (b) conditions. qz: quartz. The numerical values are the *d* values (nm) of the experimental patterns.

The 635 m sample has a R0, 35% I structure according to the present structure analysis. A major peak at 1.8 nm is associated with a broad shoulder around 2.3 nm by C_{12}-AL exchange, while the two peaks shifted to 3.7 nm by C_{18}-AL exchange (Figure 7). Peak decomposition of the C_{12}-AL-exchanged sample gives two peaks at 1.8 and 2.0 nm (Figure 10). The 656 m sample with R1, ~60% I (Table 1) showed a 3.0 nm reflection for the C_{12}-AL-exchanged sample associated with the nearly rational higher-order reflections. The C_{18}-AL-exchanged 656 m sample showed a set of integral reflections of 3.3 nm (001), 1.65 nm (002) and 1.07 nm (003). The expandability behavior is similar to those of true rectorite samples from Goto and Ohara (Figure 8 and Lagaly, 1979), though the reflections of the 656 m sample become broader and greater in *d* value than true rectorite. I-S samples with >R3, >85% I (756 m and 919 m) showed a discrete peak around 1 nm in addition to peaks at 2.45 nm and ~1.2 nm by C_{12}-AL exchange. The 2.45 nm peak is similar to that which appeared in the 635 m sample. The I-S samples with >R1, >60% I displayed a basal spacing of 3.3−3.6 nm and the rational higher-order reflections by C_{18}-AL exchange, which is similar to the behavior of the 635 m sample but not similar to macroscopic vermiculite.

The Shinzan I-S series exhibited similar expandability behavior for C_{12}-AL exchange (Figure 9) and C_{18}-AL exchange (not presented) as functions of % I and Reichweite parameters to those of Kakkonda series mentioned above. Extra peaks by C_{12}-AL exchange appeared at the low-angle side of the main peak of ~1.8 nm in all R0 samples from Shinzan. Peak decomposition of the Shinzan R0 and R1 phases, together with the Kakkonda I-S minerals, indicates that the position of extra peaks shifts gradually towards the d_{001} (2.8−3.0 nm) of R1 structure with increasing % I (Figure 10).

Li saturation

In the Li-saturation test, the layer charge arising from octahedral substitution in montmorillonite is neutralized by migration of Li ions on heating, whereas the charge arising from tetrahedral substitution in beidellite is not neutralized by the Li migration. As a result, 1.8 nm and 0.96 nm peaks after glycerol solvation are representative of beidellitic and montmorillonitic layers, respectively

(Wilson, 1987). The result of the Li-saturation tests (Figure 11) indicates that the proportion of beidellite component increases from ~0.1 in the 320 m sample to 0.55 in the 580 m sample and the 214 m sample contains ~0.2 of the beidellite component, which is consistent with the chemical analysis data (Table 1).

DISCUSSION

Characteristics of component layers in I-S

The one-dimensional XRD analysis of interstratification revealed that the Kakkonda I-S minerals are composed of three component (S, V and I) layers with variable proportions. The V-layer content is, in fact, very small throughout the I-S series. The optimized d_{001} value of the I layer is 0.998 nm and is similar to those for diagenetic I-S samples reported by Drits *et al*. (1997a) and Claret *et al*. (2004). Drits *et al*. (1997b) indicated that the d_{001} value of the I layer increases when the interlayer is occupied partly by NH_4^+ ions. The NH_4^+ ion was not detected in the Kakkonda I-S samples by preliminary Fourier transform infrared measurements (not presented). The K content of the I layer is invariably $1.6\pm0.1/O_{20}(OH)_4$ regardless of % I. The K content is smaller than that of the hypothetical end-member illite, $1.8K/O_{20}(OH)_4$, which is extrapolated from a plot of fixed K content *vs*. % I using bulk chemical analyses of I-S minerals of various origins (Meunier and Velde, 1989; Lanson and Champion, 1991; Środoń *et al*., 1992). Particles of more illitic I-S samples (*e.g*. 756 m and 919 m samples) show a lath-shaped morphology (Inoue *et al*., 2004). In general, the K content of illite is smaller in lath-shaped than in hexagonal particles (Meunier and Velde, 2004). The K content of illitic interlayer in I-S, as well as that in the end-member illite of smectite illitization, may warrant further discussion.

As for the response to alkylammonium exchange, the impurity illite present in the Goto rectorite sample did not expand with C_{12}-AL exchange. It is known that micaceous illites react very slowly with alkylammonium ions (Lagaly, 1994). If the illitic interlayer in I-S is non-expandable with C_{12}-AL exchange, sub-units of several I-layers such as III triplets and IIII quartets may behave as a segregated domain of illite present within a crystallite of I-S. This is related to the expandability behavior observed in C_{12}-AL-exchanged, 756 m and 919 m samples

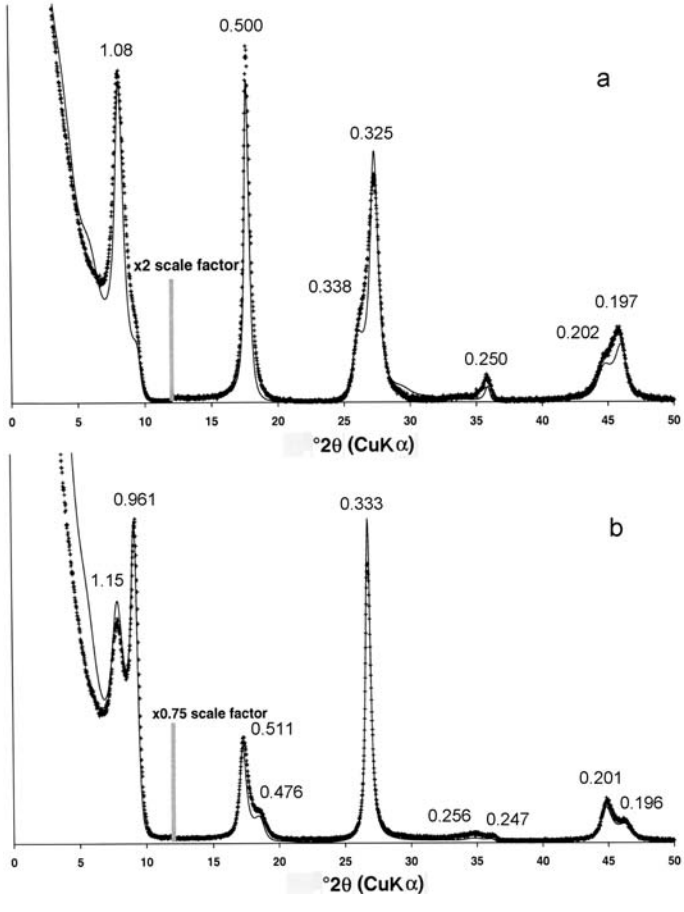

Figure 6. Comparison of experimental (+) and calculated (—) XRD patterns of sample 756 m under Ca-saturated, air-dried (a) and Ca-saturated, EG-saturated (b) conditions. The numerical values are the *d* values (nm) of the experimental patterns.

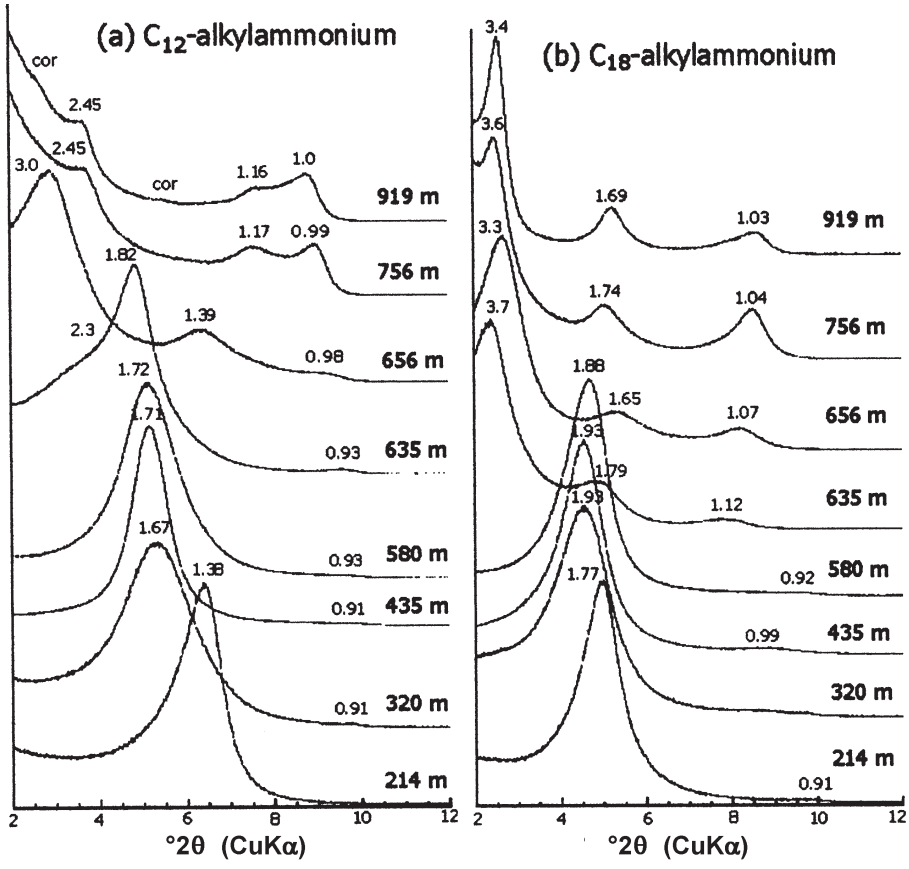

Figure 7. XRD traces of alkylammonium-exchanged specimens from Kakkonda I-S series: (a) dodecylammonium, (b) octadecylammonium, cor: corrensite.

(Figure 7). However, the illitic interlayer expands partly by C_{18}-AL exchange, and thus the C_{18}-AL exchange is inappropriate for the characterization of expandability of component layers in I-S minerals.

The S layer in the Ca-saturated Kakkonda I-S samples showed a constant expandability of 1.68 nm upon EG solvation and 1.52 nm upon air drying (Table 2). They also showed constant behavior for AL exchange so as to reflect the respective mean layer charges of $0.3-0.4/O_{10}(OH)_2$. As described previously, two peaks at 1.8 and 2.0–2.3 nm were observed in R0 I-S minerals (*e.g.* 635 m sample) by C_{12}-AL exchange as well as in the Shinzan R0 I-S minerals (Figures 7 and 10). If the sample is a stack of layers with an homogeneous layer charge, the 1.8 nm d_{001} value of the major peak can be explained either by the transition of monolayer to bilayer or by that of bilayer to pseudotrimolecular layer; the estimated layer charge is 0.38 or $0.47/O_{10}(OH)_2$, respectively, according to Olis *et al.* (1990). The layer-charge values are less than those ($<0.5/O_{10}(OH)_2$) of fully expandable S interlayer, based on the data of Christidis and Eberl (2003). The second peak of 2.0–2.3 nm by C_{12}-AL exchange corresponds to a range of layer charge, $0.56-0.71/O_{10}(OH)_2$, assuming the transition of bilayer to pseudotrimolecular layer. The layer charge is classified into that of high-charge smectite (Chiristidis and Eberl, 2003) or vermiculite. The above assignment of C_{12}-AL-exchanged XRD peaks is inconsistent with the previous XRD results in which the 635 m sample consists of 35% of I layer and 65% of S layer. The I layer has $\sim 1.6K/O_{20}(OH)_4$ and a non-expandable interlayer with C_{12}-AL exchange. Thus it is more likely that the 2.0–2.3 nm peak appearing by C_{12}-AL exchange may be derived from random interstratification of IS doublets and S layers within the crystallites. A rough estimate for the 635 m sample predicts a peak generated from the random interstratification of IS and SS doublets to appear ~2.2 nm (= (0.23/0.23 + 0.42) × 2.8 nm + (0.42/0.23 + 0.42) × 1.8 nm), assuming that the d_{001} value of an IS doublet is 2.8 nm (= 1.0 nm + 1.8 nm), that of an S layer is 1.8 nm, $W_{IS} = 0.23$ and $W_{SS} = 0.42$. This value is close to the observed one. As shown in Figure 10, the extra peak by C_{12}-AL exchange shifts towards larger d values with increasing % I, in other words, with increasing proportion of IS doublet. This supports the above interpretation. The major 1.8 nm peak by C_{12}-AL exchange is interpreted to be derived from the dominant smectitic interlayers.

The % I of 656 m I-S with R = 1, of which the % I was estimated to be 62% by Inoue *et al.* (2004), is

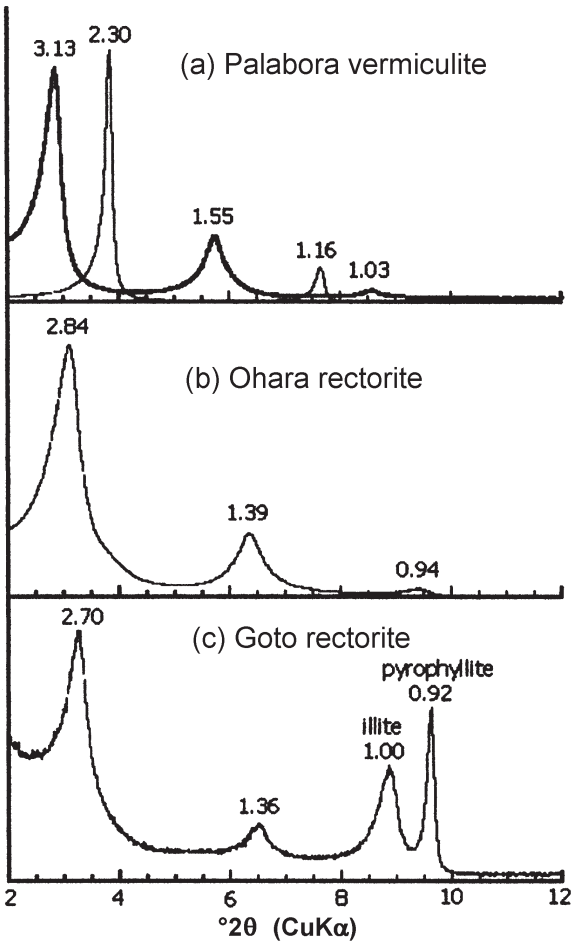

Figure 8. XRD traces of alkylammonium-exchanged vermiculite and rectorite. Thin and thick lines correspond to XRD after dodecylammonium (C_{12}) and octadecylammonium (C_{18}) exchange, respectively.

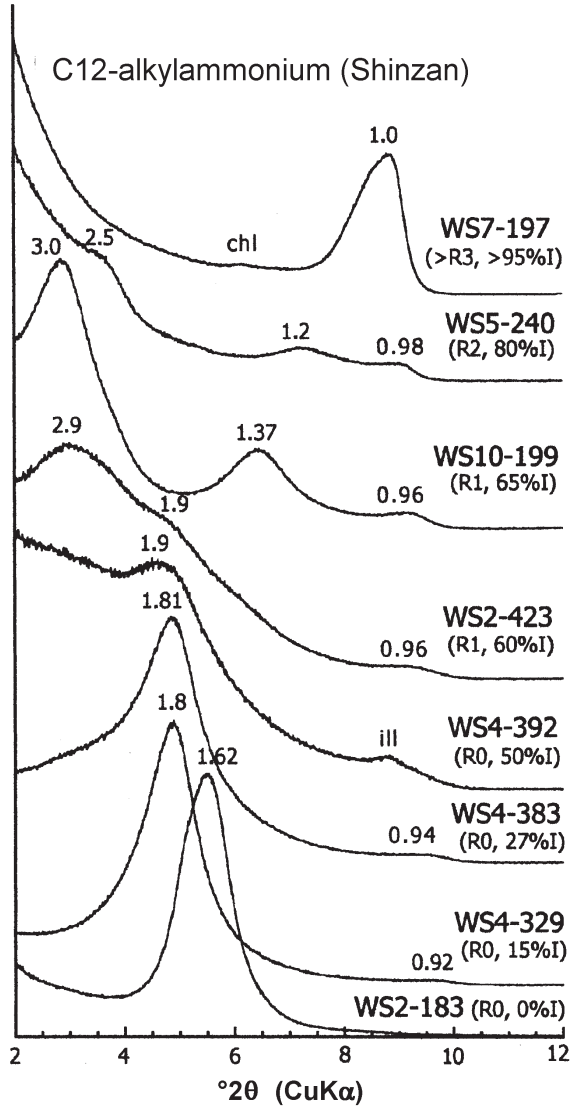

Figure 9. XRD traces of C_{12}-alkylammonium-exchanged I-S series from Shinzan. R and % I values are from Inoue *et al.* (1987). ill: illite, chl: chlorite.

somewhat larger than 50% of perfectly ordered rectorite (*i.e.* the Goto and Ohara samples). The 656 m sample contains many more II doublets and IIS triplets in crystallites compared to perfectly R1-ordered rectorite, inferred from the XRD data of the 690 m sample and the R1 phase in the 645 m sample (Table 3). This results in deviation of peak position by C_{12}-AL exchange from that of true rectorite, as shown by Lagaly (1979). The expandability behavior of >R3 I-S phases (*e.g.* the 756 m and 919 m samples) by C_{12}-AL exchange cannot be explained by the assumption of vermiculite layers because of their negligible amounts by EG saturation. Rather, the expandability behavior may be interpreted by random interstratification of several types of multiplets comprising abundant I layers and a few S layers. In conclusion, there is considerable variability in the response in expandability of the component layers in I-S, depending on the reagents used and the variability leads to ambiguity in the interpretation. We cannot obtain more accurate structural information on the AL-exchanged I-S minerals because the detailed arrangement of intercalated AL ions in the interlayer sites is unknown. Nevertheless, it is emphasized that the C_{12}-AL exchange data, in combination with the structure data by usual H_2O- and EG-saturation, provide useful information on the stacking sequence of component layers in I-S crystallites as discussed below.

The Li-saturation test of Kakkonda smectite and R0 I-S reveals that the expandability behavior of the smectitic interlayer is independent of the beidellitic layers content, at least up to 0.5.

Layer stacking model of I-S

As mentioned previously, there are two models to describe the component layers constituting the I-S interstratification: non-polar and polar 2:1 layer models

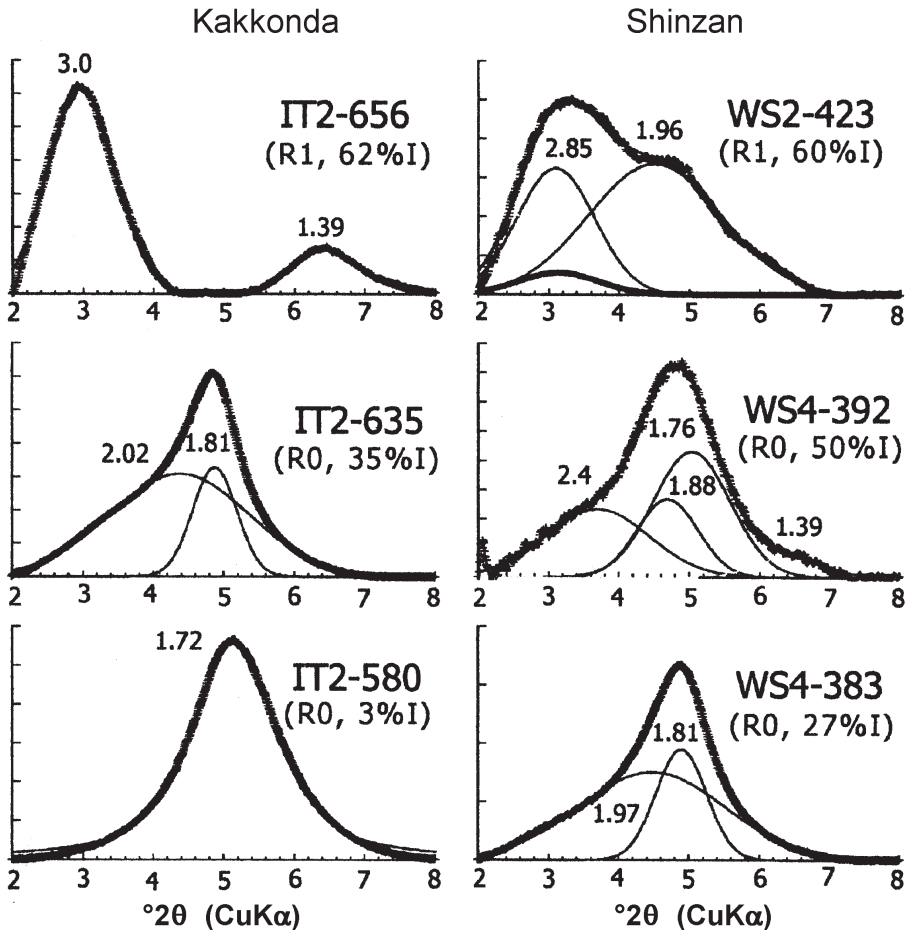

Figure 10. Decomposition of XRD patterns of C_{12}-alkylammonium-exchanged I-S minerals from Kakkonda and Shinzan. Each peak of the experimental curves (+), after subtracting the background, was decomposed by 1–4 peaks (thin curves) assuming a Gaussian shape.

(Altaner and Ylagan, 1997). Plançon (2004) demonstrated that there is no noticeable difference in simulated XRD patterns between the two models, unless the charge of the 2:1 layer is derived from the Si-Fe substitutions in tetrahedral sheets. This suggests that the structure parameters obtained in the present study may be applied to either the polar 2:1 layer model or the non-polar 2:1 layer model, though the latter model was actually used in the simulation. Previous NMR investigation of rectorite supports the polar layer model (Barron *et al*., 1985; Altaner *et al*., 1988; Jakobsen *et al*., 1995). A first-principles calculation by Stixrude and Peacor (2002) demonstrated that the polar 2:1 layer structure has a total energy lower than the non-polar structure for rectorite. Lagaly (1979) explained the expandability behavior of alkylammonium-exchanged rectorite on the polar layer model scheme. In contrast to the polar layer model, in theory, three types of interlayer sites are expected within a crystallite of I-S with 2-component layers in the non-polar layer model: a low-charge interlayer behaved as smectite, a high-charge interlayer as illite and an intermediate-charge interlayer as 'vermiculite', because the interstratification is composed of chemically homogeneous smectite and illite layers that are electrically neutral in each layer (Plançon, 2004). In fact, only negligible amounts of vermiculite layers were detected in the present XRD analysis of Kakkonda I-S minerals using the non-polar 2:1 layer model. Consequently, the interpretation of layer stacking in I-S minerals should be constructed consistently on the basis of the polar 2:1 layer model scheme regardless of % I values.

In order to describe the mode of layer stacking, we introduce a new symbol M, which is different from the Reichweite parameter. Following the polar layer model, and taking into account the occurrence probabilities of layer doublets, triplets and quartets (Table 3) and the expandability behavior by AL exchange, an I-S crystallite comprising several layers can be considered to consist of several types of sub-units (or modules) such as M0 (–SS–), M1 (–SIS–), M2 (–SIIS–), M3 (–SIIIS–), ... M*n* (–SI.....IS–), where S and I stand for the smectitic and illitic interlayers on the basis of the

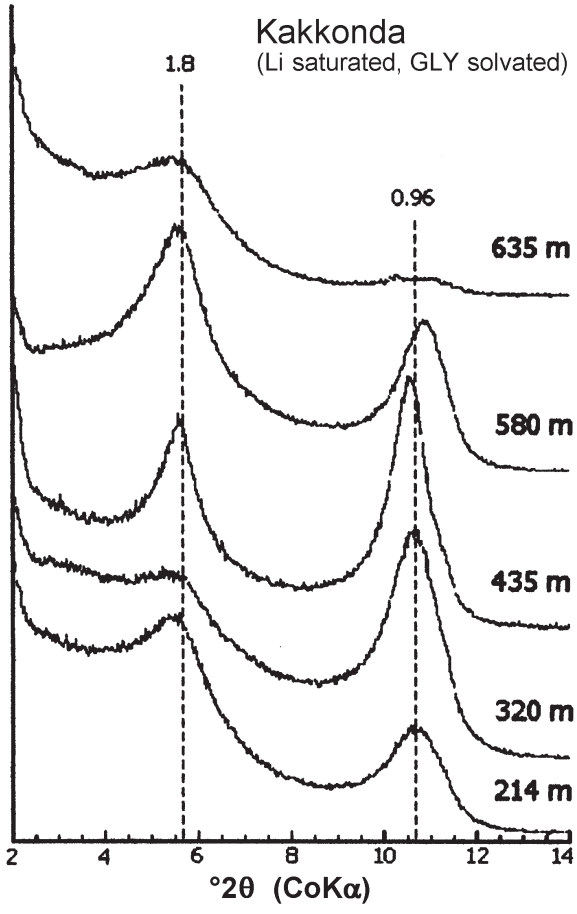

Figure 11. XRD traces of Kakkonda I-S samples after the Li-saturation test (Hofmann and Klemen, 1950).

polar 2:1 layer model. The −S and S− represent a half part of smectitic interlayer at the outermost surface and the *n* denotes the number of illitic interlayers sandwiched between two outermost smectitic surfaces. A similar model was applied to the interpretation of TEM images of I-S minerals by Bauluz *et al.* (2000). This module-stacking model may be useful in interpreting the XRD patterns of alkylammonium-exchanged I-S minerals as discussed above, as well as the HRTEM images (Murakami *et al.*, 2005) Since the ordering of I-S minerals (*i.e.* Reichweite) represents long-range ordering averaged over all layers that scatter X-rays, direct application of the module-stacking model to XRD data may be inappropriate at present. Nevertheless we infer that, for example, the occurrence probability of an IS doublet or a SIS triplet is related to that of M1 (−SIS−) type of module within an I-S crystallite. The actual modes of layer stacking will be provided by the HRTEM observations of the AL-exchanged samples (Murakami *et al.*, 2005).

Transformation of I-S minerals

The Kakkonda I-S minerals studied here are constituents of sequential smectite illitization in hydrothermally altered volcanic rocks as a function of temperature from 70 to 200ºC (Inoue *et al.*, 2004). According to the present module-stacking model, the illitization can be described as follows. The smectite precipitated at temperatures of <140ºC from solution through hydrolysis reactions of volcanic glass with meteoric water. This interpretation is supported by the textural observations and oxygen isotope measurements (Inoue *et al.*, 2004). The precipitate is a stack of the M0 type of module. The mean layer charges of product smectite (or M0 modules) are 0.3−0.4/$O_{10}(OH)_2$. The V-layer contents comprise 10% at most. The I-layer contents also are very small but occur as an M1 type of module in the crystallites with $N < 10$. As it is assumed that the composition of the original volcanic rocks and the water/rock ratio during the illitization are nearly constant at Kakkonda (Inoue *et al.*, 2004), the precipitation of modules is a function of temperature and fluid composition.

There are few occurrences of R0 I-S minerals in the studied drillhole (Inoue *et al.*, 2004). With temperature increasing only slightly to 154ºC, an R0 I-S mineral with 35% I formed at 635 m depth. The mode of layer stacking in the 635 m R0 I-S sample may be described as a mixing of M0 and M1 units. The mean layer charge of smectitic interlayer increases slightly to 0.38−0.47/$O_{10}(OH)_2$ but the K content of the illitic interlayer is constant at 1.6±0.1/$O_{20}(OH)_4$. An I-S mineral with R1 ordering, ~60% I formed at 656 m (158ºC) *via* the occurrence of a two-phase mixture of R0 and R1 structures at 645 m depth. The 656 m I-S mineral may be characterized by a mixture of dominant M1 modules and small amounts of >M2 modules, and a negligible amount of M0 module, inferred from the data of the 690 m sample. With further increasing depth and temperature, the R2 phase formed at 700 m (166ºC) and the R3 phase at 756 m (175ºC). The 756 m sample with R3, 85% I is characterized by a mixture of dominant >M2 sub-units with non-expandable illite domains. It does not contain M0 modules, and the amount of M1 module is negligible. The K ion content in the illitic interlayer of precipitating M*n* ($n \geqslant 1$) modules is systematically 1.6±0.1/$O_{20}(OH)_4$ at 70−175ºC. The above transformation is described by a stepwise precipitation of various types of modules as a function of temperature, which is compared with the consecutive change in the Reichweite from R0, R1, R2 to R3. On the other hand, a model of stepwise smectite illitization process was inferred from the TEM investigation of both diagenetic and hydrothermal I-S samples (Dong *et al.*, 1997; Bauluz *et al.*, 2000; Masuda *et al.*, 2001; Tillick *et al.*, 2001; Yan *et al.*, 2001; Bauluz *et al.*, 2002). In their model, the transformation of smectite illitization is characterized by discontinuity from smectite → R1 I-S → illite without R0, R2 and R3 I-S, using the Reichweite parameter.

From another point of view, Drits *et al.* (1997a) noted from XRD study of pelitic rocks from the North Sea that

the proportion of V layers remained constant at levels of W_V = 0.04–0.08 in the latest stage of illitization. They proposed a single interlayer transformation (SIT) mechanism *via* K fixation in the vermiculitic interlayer and succeeding transformation to illitic interlayer, which is equivalent to a layer-by-layer SST mechanism. In the Kakkonda I-S series, the V-layer content was very small as a whole and rather tended to decrease at the latest stages of illitization (Table 2). The 700 m sample has an R2 ordering, a phase considered to be relatively rare in smectite illitization (Inoue and Utada, 1983; Środoń and Eberl, 1984). It is expected that illitization by layer-by-layer SST mechanism produces R3 structure directly from R1 structure without passage *via* R2 structure (Drits, 1997). Thus the layer-by-layer transformation model via the formation of vermiculite layers is difficult to apply to the smectite illitization mechanism in hydrothermal alteration of volcanic rocks at Kakkonda. The transformation mechanism from R1 to R3 will be discussed in more detail based on the module-stacking model in part 2 (Murakami *et al*., 2005).

SUMMARY AND CONCLUSIONS

In this study, we determined the one-dimensional layer stacking sequence of I-S including the quantification of occurrence probabilities of several types of layer-doublets, layer-triplets and layer-quartets, using an I-S series from hydrothermally altered volcanic rocks. Supplementary alkylammonium exchange and Li-saturation experiments, together with the above XRD data, provided information on the expandability and stacking characteristics of the component layers in I-S minerals. The results led to the following conclusions,

(1) The XRD analysis indicated that the smectite illitization in the Kakkonda I-S minerals series occurred with a consecutive change in the R parameter from R0 to R3 in the temperature range of 70 to 175ºC.

(2) Some of the I-S minerals contained <10% vermiculite layers as the third component, but the content was small as a whole and tended to decrease with progressive illitization.

(3) The interlayer K content of the illite layer was 1.5–1.7/$O_{20}(OH)_4$ through the illitization.

(4) The C_{12}-alkylammonium-exchange experiments indicated that the layer stacking of R0-type I-S minerals is composed of IS subunits and S layers, rather than individual I and S layers. The I layers within $\geqslant$R3 I-S crystallites behaved as segregated domains for the C_{12}-alkylammonium exchange.

(5) The expandability behavior of smectite and R0 I-S is independent of the content of beidellitic layer at least up to 0.5.

Consequently, the layer stacking in I-S crystallites is consistently interpreted by introducing a new model in which the I-S crystallites consist of component modules such as M0, M1, ..., M*n* based on the polar 2:1 layer. The smectite illitization occurs with the appearance and disappearance of such modules as a function of temperature in hydrothermally altered volcanic rocks, but not by a layer-by-layer mechanism *via* K fixation in vermiculite layers. But it is apparent that the XRD results alone cannot assess the proposed model, and it must be ascertained by additional methods such as TEM investigation.

ACKNOWLEDGMENTS

We are grateful to V.A. Drits for his help in creating structure models for XRD pattern simulation and to Y. Shinohara for his providing Ohara rectorite with unpublished chemical analysis data. This manuscript was greatly improved by the comments of H. Dong, M. Krekeler and D. McCarty. Some of the experimental work was carried out during a short stay in Poitiers University and A. Inoue is grateful to CNRS, France for providing the opportunity. B. Sakharov acknowledges financial support from CNRS "poste rouge" for his stay in Grenoble. This work was partly supported by the Science Grant of the Ministry of Education, Science and Culture in Japan.

REFERENCES

Altaner, S.P. and Ylagan, R.F. (1997) Comparison of structural models of mixed-layer illite/smectite and reaction mechanisms of smectite illitization. *Clays and Clay Minerals*, **45**, 517–533.

Altaner, S.P., Weiss, C.A. Jr. and Kirkpatrick, R.J. (1988) Evidence from ^{29}Si NMR for the structure of mixed-layer illite/smectite clay minerals. *Nature*, **331**, 699–702.

Amouric, M. and Olives, J. (1991) Illitization of smectite as seen by high-resolution transmission electron microscopy. *European Journal of Mineralogy*, **3**, 831–835.

Barron, R.F., Slade, P. and Frost, R.L. (1985) Ordering of aluminium in tetrahedral sites in mixed-layer 2:1 phyllosilicates by solid-state high-resolution NMR. *Journal of Physical Chemistry*, **89**, 3880–3885.

Bauluz, B., Peacor, D.R. and Gonzalez Lopez, J.M. (2000) Transmission electron microscopy study of illitization in pelites from the Iberian Range, Spain: layer-by-layer replacement? *Clays and Clay Minerals*, **48**, 374–384.

Bauluz, B., Peacor, D.R. and Ylagan, R.F. (2002) Transmission electron microscopy study of smectite illitization during hydrothermal alteration of a rhyolitic hyaloclastite from Ponza, Italy. *Clays and Clay Minerals*, **50**, 157–173.

Christidis, G.E. and Eberl, D.D. (2003) Determination of layer-charge characteristics of smectites. *Clays and Clay Minerals*, **51**, 644–655.

Claret, F., Sakharov, B.A., Drits, V.A., Velde, B., Meunier, A., Griffault, L. and Lanson, B. (2004) Clay minerals in the Meuse-Haute Marne underground laboratory (France): Possible influence of organic matter on clay mineral evolution. *Clays and Clay Minerals*, **52**, 515–532.

Dong, H., Peacor, D.R. and Freed, R.L. (1997) Phase relations among smectite, R1 illite-smectite, and illite. *American Mineralogist*, **82**, 379–391.

Drits, V.A. (1997) Mixed-layer minerals. Pp. 153–190 in: *Modular Aspects of Minerals* (S. Merlino, editor). EMU Notes in Mineralogy, **1**, Eötvös University Press, Budapest.

Drits, V.A. and Tchoubar, C. (1990) *X-ray Diffraction by Disordered Lamellar Structures*. Springer-Verlag, Berlin, 371 pp.

Drits, V.A., Lindgreen, H., Sakharov, B.A. and Salyn, A.S. (1997a) Sequence structure transformation of illite-smectite-vermiculite during diagenesis of Upper Jurassic shales, North Sea. *Clay Minerals*, **33**, 351–371.

Drits, V.A., Lindgreen, H. and Salyn, A.L. (1997b) Determination of the content and distribution of fixed ammonium in illite-smectite by X-ray diffraction: Application to North Sea illite-smectite. *American Mineralogist*, **82**, 79–87.

Hofmann, U. and Klemen, R. (1950) Verlust der Austauschfahigeit von Lithiumionen an Bentonit durch Erhitzung. *Zeitschrift fur Anorganische Chemie*, **262**, 95–99.

Howard, S.A. and Preston, K.D. (1989) Profile fitting of powder diffraction patterns. Pp. 217–275 in: *Modern Powder Diffraction* (D.L. Bish and J.E. Post, editors). Reviews in Mineralogy, **20**, Mineralogical Society of America, Washington, D.C.

Hower, J., Eslinger, E.V., Hower, M.E. and Perry, E.A. (1976) Mechanism of burial metamorphism of argillaceous sediments: Mineralogical and chemical evidence. *Geological Society of America Bulletin*, **87**, 725–737.

Inoue, A. (1984) Thermodynamic study of Na-K-Ca exchange reactions in vermiculite. *Clays and Clay Minerals*, **32**, 311–319.

Inoue, A. and Utada, M. (1983) Further investigations of a conversion series of dioctahedral mica/smectites in the Shinzan hydrothermal alteration area, northeast Japan. *Clays and Clay Minerals*, **31**, 401–412.

Inoue, A., Minato, H. and Utada, M. (1978) Mineralogical properties and occurrence of illite/montmorillonite mixed layer minerals formed from Miocene volcanic glass in Waga-Omono district. *Clay Science*, **5**, 123–136.

Inoue, A., Kohyama, N., Kitagawa, R. and Watanabe, T. (1987) Chemical and morphological evidence for the conversion of smectite to illite. *Clays and Clay Minerals*, **35**, 111–120.

Inoue, A., Bouchet, A., Velde, B. and Meunier, A. (1989) Convenient technique for estimating smectite layer percentage in randomly interstratified illite/smectite minerals. *Clays and Clay Minerals*, **37**, 227–234.

Inoue, A., Watanabe, T., Kohyama, N. and Brusewitz, A.M. (1990) Characterization of illitization of smectite in bentonite beds at Kinnekulle, Sweden. *Clays and Clay Minerals*, **34**, 241–249.

Inoue, A., Hara, J. and Imai, A. (2001) Genesis of Na-series rock alteration widespread in the southeastern area of Hachimantai geothermal field: water-rock interactions driven by descending groundwater and fossil seawater. *Shigen-Chishitsu* (*Journal of Society of Resource Geology, Japan*), **51**, 101–120 (in Japanese).

Inoue, A., Meunier, A. and Beaufort, D. (2004) Illite-smectite mixed-layer minerals in felsic voclaniclastic rocks from drill cores, Kakkonda, Japan. *Clays and Clay Minerals*, **52**, 66–84.

Jagodzinski, H. (1949) Eindimensionale fehlordnung in hristallen und ihr einfluss auf die Rontgeninterferenzen. I. Berechnung des fehlordnungsgrades au der Rontgenintensitaten. *Acta Crystallographica*, **2**, 201–207.

Jakobsen, H.J., Nielsen, N.C. and Lindgreen, H. (1995) Sequences of charged sheets in rectorite. *American Mineralogist*, **80**, 247–252.

Keller, W.D., Reynolds, R.D., Jr. and Inoue, A. (1986) Morphology of clay minerals in the smectite-to-illite conversion series by scanning electron microscopy. *Clays and Clay Minerals*, **34**, 187–197.

Lagaly, G. (1979) The 'layer charge' of regular interstratified 2:1 clay minerals. *Clays and Clay Minerals*, **27**, 1–10.

Lagaly, G. (1994) Layer charge determination by alkylammonium ions. Pp. 1–46 in: *Layer Charge Characteristics of 2:1 Silicate Clay Minerals* (A.R. Mermut, editor). CMS Workshop Lectures, **6**, The Clay Minerals Society, Boulder, Colorado.

Lanson, B. (1997) Decomposition of experimental X-ray diffraction patterns (profile fitting): a convenient way to study clay minerals. *Clays and Clay Minerals*, **45**, 132–146.

Lanson, B. and Champion, D. (1991) The I/S-to-illite reaction in the late stage diagenesis. *American Journal of Science*, **291**, 473–506.

Masuda, H., Peacor, D.R. and Dong, H. (2001) Transmission electron microscopy study of conversion of smectite to illite in mudstones of the Nankai Trough: Contrast with coeval bentonites. *Clays and Clay Minerals*, **49**, 109–118.

Meunier, A. and Velde, B. (1989) Solid solution in illite/smectite mixed layer minerals and illite. *American Mineralogist*, **74**, 1106–1112.

Meunier, A. and Velde, B. (2004) *Illite*. Springer, Berlin, 286 pp.

Meunier, A., Lanson, B. and Beaufort, D. (2000) Vermiculitization of smectite interfaces and illite layer growth as a possible dual model for illite-smectite illitization in diagenetic environments: a synthesis. *Clay Minerals*, **35**, 573–586.

Murakami, T., Inoue, A., Lanson, B., Meunier, A. and Beaufort, D. (2005) Illite-smectite mixed-layer minerals in hydrothermal alteration of volcanic rocks: II. One-dimensional HRTEM structure-images and formation mechanism. *Clays and Clay Minerals*, **53**, 440–451.

Olis, A.C., Malla, P.B. and Douglas, L.A. (1990) The rapid estimation of the layer charges of 2:1 expanding clays from a single alkylammonium ion expansion. *Clay Minerals*, **25**, 39–50.

Olives, J., Amouric, M. and Perbost, R. (2000) Mixed layering of illite-smectite: Results from high-resolution transmission electron microscopy and lattice-energy calculations. *Clays and Clay Minerals*, **48**, 282–289.

Plançon, A. (2004) Consistent modeling of the XRD patterns of mixed-layer phyllosilicates. *Clays and Clay Minerals*, **52**, 47–54.

Sakharov, B.A., Lindgreen, H., Salyn, A. and Drits, V.A. (1999) Determination of illite-smectite structures using multispecimen X-ray diffraction profile fitting. *Clays and Clay Minerals*, **47**, 555–566.

Środoń, J. and Eberl, D. D. (1984) Illite. Pp. 495–544 in: *Micas* (S.W. Bailey, editor). Reviews in Mineralogy, **13**, Mineralogical Society of America, Washington D.C.

Środoń, J., Elsass, F., MacHardy, W. J. and Morgan, D.J. (1992) Chemistry of illite-smectite inferred from TEM measurements of fundamental particles. *Clay Minerals*, **27**, 137–158.

Stixrude, L. and Peacor, D.R. (2002) First-principles study of illite-smectite and implications for clay mineral systems. *Nature*, **420**, 165–168.

Tillick, D.A., Peacor, D.R. and Mauk, J.L. (2001) Genesis of dioctahedral phyllosilicates during hydrothermal alteration of volcanic rocks: I. The Golden Cross epithermal ore deposit, New Zealand. *Clays and Clay Minerals*, **49**, 126–140.

Veblen, D.R., Guthrie, G.D., Livi, K.J.T. and Reynolds, R.C. Jr. (1990) High-resolution transmission electron microscopy and electron diffraction of mixed-layer illite/smectite: Experimental results. *Clays and Clay Minerals*, **38**, 1–13.

Watanabe, T. (1988) The structure model of illite/smectite interstratified mineral and the diagram for its identification. *Clay Science*, **7**, 97–114.

Wilson, M.J. (1987) X-ray powder diffraction methods. Pp. 26–98 in: *A Handbook of Determinative Methods in Clay Mineralogy* (M. J. Wilson, editor), Blackie, Glasgow, UK.

Yan, Y., Tillick, D.A., Peacor, D.R. and Simmons, S.F. (2001) Genesis of dioctahedral phyllosilicates during hydrothermal alteration of volcanic rocks: II. The Broadlands-Ohaaki hydrothermal system, New Zealand. *Clays and Clay Minerals*, **49**, 141–155.

(*Received 2 August 2004; revised 6 June 2005; Ms. 945; A.E. Douglas K. McCarty*)